APPROVAL SHEET

Title of Thesis: A Bifurcational Analysis of the Onset of Type 1 Diabetes

Name of Candidate: Adam Reddan
Applied Mathematics, 2018

Thesis and Abstract Approved: _____

Doctor Bradford Peercy
Associate Professor
Department of Mathematics and
Statistics

Date Approved: _____

ABSTRACT

Title of dissertation: A BIFURCATIONAL ANALYSIS
OF THE ONSET OF TYPE ONE DIABETES

Adam Reddan, Master of Science Mathematics, 2018

Dissertation directed by: Professor Bradford Peercy
Department of Mathematics

The purpose of this paper is to combine two models of diabetes and analyze the periodic behavior and the bifurcations produced by the newly combined model. The first of these two models by Mahaffy [1] analyzes the onset of type 1 diabetes (T1D) at the cellular level due to an imune response, where as the second, the Topp model [2], analyzes the coupled dynamics between beta cell mass, insulin, and glucose. Both models include an equation for beta cell mass which is the key equation in combining the two and will enable us to look at how insulin and glucose levels change and relate to the onset of T1D. The resulting model provides a plethora of mathematically interesting properties such as various different bifurcations and bifurcation types as well as chaos. In terms of biology, we show that the combined model produces a situation in which beta cells actually recover after the initial attack on the pancreas. We are able look at the concentration of certain cell types in the blood at different stages during the onset. Our goal is to use the mathematical properties mentioned above to conclude that the combination of the Mahaffy and Topp models, and thus coupling glucose and insulin to immune cells, leads to a case of recovery of beta cells as well as forcing beta cell recovery by controlling the degradation of beta cell peptides. This exhibits the impact that certain parameter changes have on pathways to T1D. From

this analysis, we can conclude that there are two types of recovery from T1D before it sets in and becomes permanent. The first is cyclic recovery in which beta cell mass, insulin concentrations, and glucose concentrations oscillate as they return to their healthy steady state values and low levels of effector T-cells remain in the blood stream but not high enough levels to induce full blown T1D. The second is noncyclic recovery in which beta cell mass, insulin concentrations, and glucose concentrations return to healthy steady state values but do not oscillate, which means that no effector T-cells remain in the blood after a certain time period.

A Bifurcational Analysis of the Onset of Type 1 Diabetes

Adam Reddan

December 17, 2018

Table of Contents

List of Tables

List of Figures

Chapter 1: Introduction

Type 1 Diabetes (T1D) is an autoimmune disease in which the body's own immune system targets and kills the insulin producing beta cells in the pancreas resulting in dangerously high blood sugar levels. Individuals with this disease are typically diagnosed during adolescence and thus face a life time of impaired health of all forms, such as kidney failure, blindness, amputation due to infection, and more, hence our motivation for studying its behavior. While no known cure exists for T1D there are many treatments for it. Each involve injecting insulin of some kind multiple times a day if not having it constantly supplied.

In T1D, T-cells play a significant role. T-cells mature in the thymus where they cross react with self-proteins are normally eliminated in order to prevent autoimmunity. From here they travel to the lymph nodes where they interact with antigen presenting cells (APCs). These consist of a peptide held in a larger protein called a Major Histocompatibility Complex (MHC). The peptide-MHC complex or p-MHC interacts with receptors on the surface of the T-cells (TCRs) to activate and initiate the immune response. Normally the APCs display antigens that come from foreign proteins such as from bacteria or viruses. However in T1D the antigen proteins come from the individual's own body which can be triggered by infection or another injury initiating the disease. Once this process begins there is no known way of stopping it since the targeted beta cells will produce peptides with the same self-antigen causing an endless cycle of beta cell destruction.

The model that will be the main focus of this paper comes from two independent models that come from [1] and [2] and will be briefly described in the next section. Alone the Mahaffy model only captures T1D itself at the cell population level while leaving out important information and feedback regarding both insulin and glucose. At the same time the Topp model is mostly used to model Type 2 Diabetes and therefore takes no information into account regarding the destruction of beta cells by the immune system. Our aim is to combine these two models in such a way as to include the effects that an autoimmune response has on blood glucose levels and the effects that blood glucose levels can have on the autoimmune response via the production of beta cells in response to elevated glucose levels.

Combining these two models leads to the highly complicated and nonlinear behavior of the immune system itself, not to mention one with inappropriate responses to certain stimuli, the two individual models as well as the combined model provides a plethora of bifurcations and interesting trajectories.

Chapter 2: An Introduction to the Two Pre-Existing Models

Below are the two models that were combined to obtain our results. The Mahaffy Model captures the cellular behavior of the immune system as autoimmunity sets in and destroys beta cells. The Topp Model models the dynamics of beta cells mass and long-time average concentrations of glucose and insulin concentrations in the blood. Since both models capture the dynamics of beta cell mass and are single compartment models they were easily combined to produce the results we discuss via the beta cell equation in each model.

2.1 The Mahaffy Model

The Mahaffy Model [1] combines activated, memory, and effector T-cells along with beta cell peptides and beta cell mass, equation (2.1) describes the rate at which T-cells are being activated.The rate at which activated T-cells become memory cells i.e. the rate at which activated T-cells fail to locate and destroy a beta cell is described by equation (2.2). The rate at which activated T-cells effectively seek out and destroy beta cells thus allowing T1D to progress and eventually settle in is given by equation (2.3). The rate of change in peptide accumulation levels, equation (2.4) describes how many peptides will be available to activate T-cells to seek out beta cells. The rate of change of the remaining population of beta cells is given by equation (2.5). See Table 1.1 and 1.2 in Appendix 1 for default values and definitions of parameters. Only the parameter R will differ from the Mahaffy Model in Table 1.1 and the reasoning behind this will be discussed when the two models are combined. For the Mahaffy Model alone the default value is $R = 50 \times 10^{-6} cells^{-1} days^{-1}$ and has the same meaning as is stated in Table 1.1. The Mahaffy Model is quite sensitive to changes in parameters e.g. changing δ_P, as well as many other parameters, causes cyclic oscillations in $A(t), M(t)$, and $E(t)$ and the cyclic decay of beta cells. Many of these parameters, such as δ_P and ϵ lead to Hopf bifurcations. The Mahaffy Model is

$$\frac{dA}{dt} = (\sigma_1 + \alpha_1 M) f_1(p) - (\beta + \delta_A) A - \epsilon A^2, \tag{2.1}$$

$$\frac{dM}{dt} = \beta 2^{m_1} f_2(p) A - f_1(p) \alpha_1 M - \delta_M M, \tag{2.2}$$

$$\frac{dE}{dt} = \beta 2^{m_2} (1 - f_2) A - \delta_E E, \tag{2.3}$$

$$\frac{dp}{dt} = REB - \delta_p p, \tag{2.4}$$

$$\frac{dB}{dt} = -\hat{k} EB, \tag{2.5}$$

where

$$f_1(p) = \frac{p^n}{k_1^n + p^n}, \tag{2.6}$$

$$f_2(p) = \frac{\hat{a} k_2^m}{k_2^m + p^m}. \tag{2.7}$$

For the Hill functions (2.6) and (2.7) we have $n, m, k_1, k_2 > 0$, and $0 < \hat{a} < 1$. Equation (2.6) is the fraction of incoming naive T-cells and memory T-cells that become activated. Lastly, for the Mahaffy Model, we turn our attention to (2.7) which separates the activated T-cells into f_2 memory cells and $(1 - f_2)$ effector cells which depend on the number of peptides produced by the destroyed beta cells.

2.2 The Topp Model

The Topp Model [2] describes the dynamics of the insulin glucose system and include how the feed back from glucose effects beta cell mass. The equations are:

$$\frac{dB}{dt} = (-r_2 G^2 + r_1 G - d_0) B, \tag{2.8}$$

$$\frac{dI}{dt} = \sigma_2 B \frac{G^2}{\alpha_2 + G^2} - kI, \tag{2.9}$$

$$\frac{dG}{dt} = R_0 - (E_{GO} + SI) G. \tag{2.10}$$

where $B(t)$ is the beta cell mass, $I(t)$ is the concentration of insulin in the blood, and $G(t)$ is the concentration of glucose in the blood all at time t. The terms in (2.8) describe how glucose concentration effects the rate of change in beta cell mass. For example, the term $-r_2G^2$ tells us that for very high concentrations of glucose beta cell mass will decrease at a rate proprtional to G^2 (with proportionality rate constant r_2)the term r_1G tells us that for intermediate values of glucose concentration beta cell mass will rise linearly with glucose with rate constant r_1 and the term d_0 tells us how fast beta cell mass decreases at zero glucose. The first term in (2.9), $\sigma_2 B\frac{G^2}{\alpha_2+G^2}$, describes insulin secretion with maximum value $\sigma_2 B$ and the second term, $-kI$ describes the insulin cleared in the blood. Lastly equation (2.10) represents the change in glucose concentration which is equal to glucose production minus glucose uptake. The parameter R_0 is the net rate of production at zero glucose and the term $(E_{GO} + SI)G$ is the insulin-independent and insulin-sensitive glucose uptake. The difference in equation (2.10) is the balance between these two processes. The Topp Model also has saddle node bifurcation for the parameters r_1, r_2, and d_0 each of which represent a pathway to T1D [2]. This model exhibits the bistability of the healthy steady state and diseased steady state for beta cell mass.

2.3 The Combined Model

We can define the common term for beta cell mass to combine the two models into the one seen below where all parameters and variables have the same meanings defined above. See Appendix 1, Table 1.1 for parameter meanings and default values as well as Table 1.6 for

variable meanings and units. We now arrive at the combined model:

$$\frac{dA}{dt} = (\sigma_1 + \alpha_1 M) f_1(p) - (\beta + \delta_A) A - \epsilon A^2, \tag{2.11}$$

$$\frac{dM}{dt} = \beta 2^{m_1} f_2(p) A - f_1(p) \alpha_1 M - \delta_M M, \tag{2.12}$$

$$\frac{dE}{dt} = \beta 2^{m_2} (1 - f_2) A - \delta_E E, \tag{2.13}$$

$$\frac{dp}{dt} = REB - \delta_p p, \tag{2.14}$$

$$\frac{dB}{dt} = (-r_2 G^2 + r_1 G - d_0 - \hat{k} E) B, \tag{2.15}$$

$$\frac{dI}{dt} = \sigma_2 B \frac{G^2}{\alpha_2 + G^2} - kI, \tag{2.16}$$

$$\frac{dG}{dt} = R_0 - (E_{GO} + SI) G, \tag{2.17}$$

$$f_1(p) = \frac{p^n}{k_1^n + p^n}, \tag{2.18}$$

$$f_2(p) = \frac{a k_2^m}{k_2^m + p^m}. \tag{2.19}$$

It is important to note that the value of R has been changed from $R = 50 \times 10^{-6}$ to $R = (50/300) \times 10^{-6}$, due to the difference in the units used by Topp and Mahaffy to quantify the change in beta cells. This change makes it so that beta cells are now being measured in mg/dl throughout the combined model so that the healthy steady state does in fact occur at a physiologically meaningful value $B = 300$ mg/dl.

Since the scale of the equations in the combined model vary in their orders of magnitude by a significant amount we will be using the nondimensionalized model, described in section 2.3.1, for our bifurcation diagrams. We also use the quasi-steady state assumption $\frac{dI}{dt} = 0$ instead of $\frac{dp}{dt} = 0$. This will be justified and further explained in the results section.

2.3.1 The Nondimensionalized Combined Model

By making the substitutions $t = \mathring{a}\tau, A = \bar{a}a, M = \bar{m}m, E = \bar{e}e, P = \bar{\rho}\rho, B = \bar{b}b, I = \bar{i}i$, and $G = \bar{g}g$ with $\mathring{a} = 1, \bar{a} = \frac{1}{\epsilon\mathring{a}}, \bar{m} = \bar{a}\mathring{a}\beta 2^{m_1}, \bar{e} = \bar{a}\mathring{a}\beta 2^{m_2}, \bar{p} = R\mathring{a}\bar{e}\bar{b}, \bar{b} = 300, \bar{i} = 10,$

$\bar{g} = \sqrt{\alpha_2}$ and by defining $c_{14} = \frac{\mathring{a}R_0}{\sqrt{\alpha_2}}$, one obtains the following nondimensionalized form of the combined model. See appendix 1, Table 1.4 for parameter definitions and default values:

$$a' = (c_1 + c_2 m) f_1(\rho) - c_3 a - a^2, \tag{2.20}$$

$$m' = f_2(\rho) a - c_4 f_1 m - c_5 m, \tag{2.21}$$

$$e' = (1 - f_2(\rho)) a - c_6 e, \tag{2.22}$$

$$\rho' = eb - c_7 \rho, \tag{2.23}$$

$$b' = b(-c_8 g^2 + c_9 g - c_{10} - c_{11} e), \tag{2.24}$$

$$i' = c_{12} b \frac{g^2}{1 + g^2} - c_{13} i, \tag{2.25}$$

$$g' = c_{14} - (c_{15} + c_{16} i) g, \tag{2.26}$$

$$f_1(\rho) = \frac{\rho^{c_{17}}}{c_{18}^{c_{17}} + \rho^{c_{17}}}, \tag{2.27}$$

$$f_2(\rho) = \frac{c_{19} c_{20}^{c_{21}}}{c_{20}^{c_{21}} + \rho^{c_{21}}} \tag{2.28}$$

This form of the combined model makes it much easier to analyze and construct the bifurcation diagrams and figures however our analysis will be done on equations (2.11)-(2.19).

Chapter 3: Geometric Reduction of the Combined Model to Observe Steady State Solutions

This section is devoted to describing the methods used to find the equilibrium points for the combined model,(2.11) - (2.19), and then to present the results. We begin by setting the left hand side of every equation in the Combined Model equal to 0 and assuming that $B \neq 0$. This is the crucial first step as it allows one to solve for G in terms of just E. We start by noticing that now (2.15) is quadratic in G so via the quadratic formula we have

$$G_{\pm}(E) = \frac{r_1 \pm \sqrt{r_1^2 - 4r_2(d_0 + \hat{k}E)}}{2r_2}. \tag{3.1}$$

From this point on whenever we have a function with $\pm$ in it we will emphasize whether the $+$ equation or the $-$ equation is being referred to by a subscript on the dependent variable such as $G_+(E)$. Similarly one can use equation (2.17) to solve for insulin in terms of glucose to get

$$I_{\pm}(E) = I(G_{\pm}(E)) = \frac{R_0 - E_{GO}G_{\pm}(E)}{SG_{\pm}(E)}. \tag{3.2}$$

Now by plugging both (3.1) and (3.2) into (2.16) and solving for B we obtain our first important function:

$$B_{\pm}(E) = \frac{kI_{\pm}(E)(\alpha_2 + G_{\pm}^2(E))}{\sigma_2 G_{\pm}^2(E)}. \tag{3.3}$$

Now we begin to derive a separate function $H(E, B)$. We start with the left hand side of every equation in the Combined Model set equal to 0 again and use equation (2.14) to get:

$$p(E, B) = \frac{REB}{\delta_p}, \tag{3.4}$$

which now gives us via (2.18) and (2.19)

$$f_1(E, B) = \frac{(\frac{REB}{\delta_p})^n}{k_1^n + (\frac{REB}{\delta_p})^n} \tag{3.5}$$

$$f_2(E, B) = \frac{ak_2^m}{k_2^m + (\frac{REB}{\delta_p})^m}. \tag{3.6}$$

From here we can solve equation (2.12) for M in terms of A to get

$$M(A, p(E, B)) = \frac{\beta 2^{m_1} f_2 A}{\alpha_1 f_1 + \delta_M}. \tag{3.7}$$

Now by plugging (3.7) into (2.11) we obtain a quadratic in terms of A. So by the quadratic formula we have:

$$A_{\pm}(E, B) = \frac{-b \pm \sqrt{b^2 - 4ac}}{2a}, \tag{3.8}$$

where

$$a = -\epsilon,\ b = \frac{f_1 f_2 \alpha_1 \beta 2^{m_1}}{\alpha_1 f_1 + \delta_M} - (\beta + \delta_A),\ c = f_1 \sigma_1.$$

Then finally by plugging (3.8) into (2.13) we obtain the implicit function of E in terms of E and B

$$H_{\pm}(E, B) = \beta 2^{m_2}(1 - f_2(E, B))A_{\pm}(E, B) - \delta_E E. \tag{3.9}$$

It is important to note that only $H(E, B) = 0$ is of interest. Now that we have (3.3) and (3.9) we can use them to verify that the combined model will reduce to the Mahaffy and Topp models respectively when decoupled. To see this first set $B = 300$, since we have normalized B to be 300 instead of 1,as was done by Mahaffy [1], in (3.9). As one can verify

using the "Boot Method", discussed in the next section, we have $H(E, B^*) = H(E) = 0$ for $E = 0, E = 11622$, and $E = 35562$ for $B^* = 0, 36.96$, and 300, respectively. We have that the three values of E correspond to the three equilibrium points for the Mahaffy Model. After plugging these values into equations (3.8) and (3.7) we recover the same three equilibrium points in the reduced AME model discussed in the Mahaffy paper confirming that the combined model successfully reduces to the Mahaffy model when decoupled. It is important to note that these equilibrium values in the AME model were scaled down by $\bar{A} = 10^3, \bar{M} = 10^4, \bar{E} = 10^6$.

Now consider equation (3.3) where $\hat{k} = 0$. Since the term $-\hat{k}E$ is the only term in it that differs from the original Topp Model setting it equal to 0 decouples the full model isolating the last three equations as the Topp model. To check this we set $\hat{k} = 0$ in (3.3) and plot the results. As one can see from Figure 3.1 we get two nontrivial equilibrium points that match the two nontrivial equilibrium points obtained in [2]. To verify the third equilibrium point simply assume that B=0 and plug it into (2.16) to get I=0 and then plug that into (2.17) to get the same diseased steady state as Topp et al. Thus showing that one can recover both the Mahaffy Model and the Topp Model by making certain changes in parameters.

3.1 Equilibrium Points and Stability Analysis

The equations derived in the previous section are of particular use when finding equilibrium points too. Before proceeding one can simplify the work we are about to do by noticing that $H_+(E, B) < 0$ for all (E, B) and can therefore be ignored. By plotting both $B_\pm(E)$ and $H_-(E, B) = 0$ together, see Figure 3.2 and Figure 3.3, one finds six points of intersection between the curves of equation (3.3) with the contours of $H_-(E) = 0$ at $(E, B) = (0, 300), (11.753, 296.54), (74567, 134.34)$,

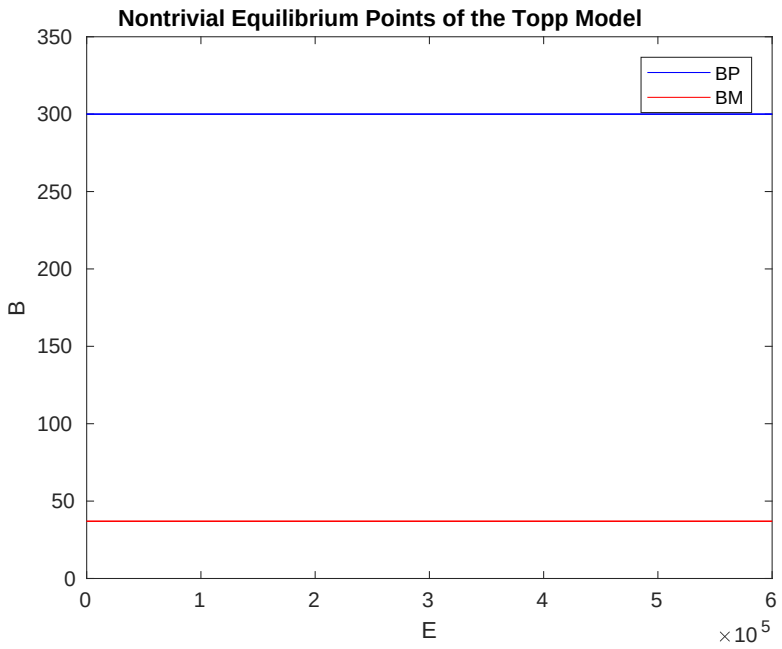

Figure 3.1: This is a plot of $BP = B_+(E)$ and $BM = B_-(E)$ when $\hat{k} = 0$. As one can see $B_+(E) = 300$ which corresponds to the healthy steady state and $B_-(E) = 36.96$ which corresponds to the threshold steady state. $B = 0$ is the diseased steady state (not shown) $(0, 36.96), (95.607, 38.23)$, and $(77913.936, 128.2)$.

Since the curve $H_\pm(E, B) = 0$ represents all points (E,B) such that the Mahaffy terms equal zero and the values of $B_\pm(E)$ represent the values of E that make the terms from the Topp model zero each point of intersection represents a nontrivial equilibrium point for the full model. Using the six points in the EB plane mentioned above we can use $A_-(E, B), M_-(E, B), p(E, B), I_\pm(E), G_\pm(E)$ to find the values of A,M,p,I, and G that correspond to each of the six points of intersection. One must be careful to make sure that the correct forms of $I_\pm(E), G_\pm(E)$ are used when finding the values that correspond to a point of intersection, if the curve comes from B_- then the minus form of the equations must

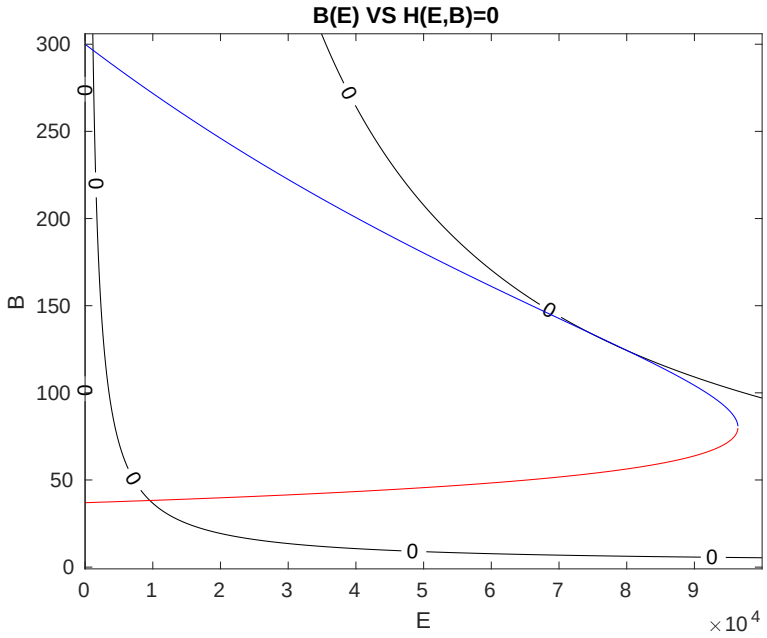

Figure 3.2: This is a plot of $B_{\pm}(E)$ and $H(E,B) = 0$. The black curve is the contour of $H_{+}(E,B) = 0$, the blue curve is $B_{+}(E)$, and the red curve is $B_{-}(E)$. Since each point of intersection with the contour of $H(E,B) = 0$ is a steady state we can clearly see two equilibrium points together with what appears to be a point of tangency but is in fact two distinct points of intersection. See Figure 3.3. We also have that $(0, B_{\pm}(0))$ as two more equilibrium points.

also be used where as only the minus form of the Mahaffy equations will be used since the plus forms gives negative values only. By plugging each point of intersection into the appropriate equations one obtains the nontrivial equilibrium points for the full model. Lastly one can solve for the seventh and final equilibrium point of interest by simply setting B=0 and solving for each variable by hand in the full model to obtain the equilibrium point $(A, M, E, p, B, I, G) = (0, 0, 0, 0, 0, 0, 600)$.

We now describe the method used to numerically solve for the steady states of the combined model. When finding the values of E and B for which $B_{\pm}$ and $H_{\pm}(E,B)$ intersect

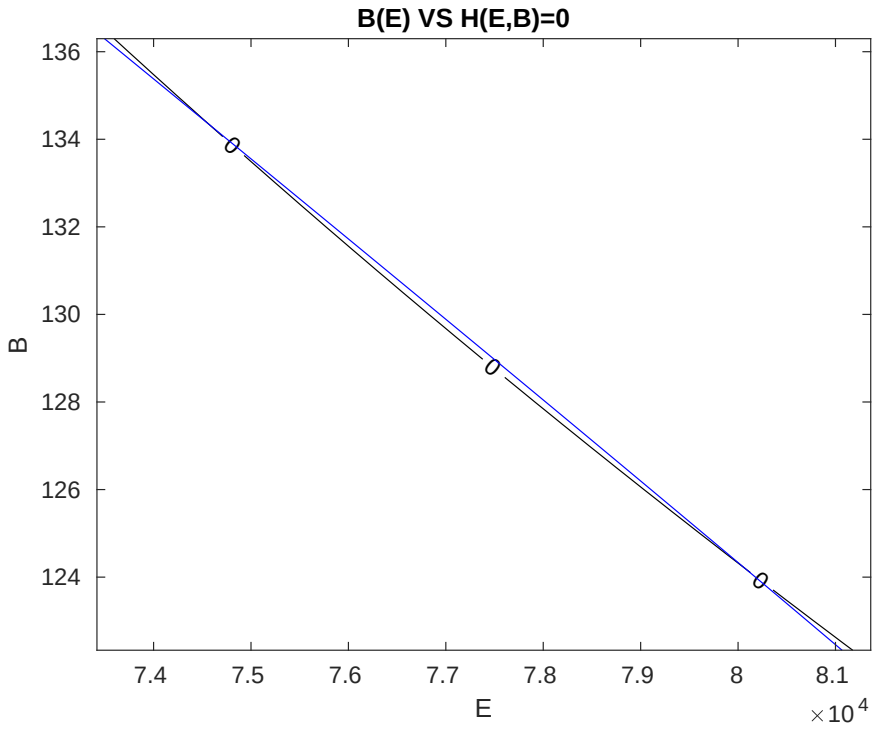

Figure 3.3: This figure is a closer view of EQ PTS III and VI since they occur too close together to be seen in figure 2

one must make an initial guess for B^* and E based on Figures 3.2 and 3.3 and use matlab's fsolve function to output the accurate value of E at the point of intersection closest to the initial guess for B. (BetterZeros.m). From here enter the newly obtained value of E into either B_+ or B_- (BetterEBPlots.m). This will produce the actual value of B at the point of intersection. From here using the equations mentioned above one can accurately find all other variable values at each of the seven equilibrium points by entering the values of E and B for A,M,E,p,B,I, and G just found (BetterEBPlots.m). The stability for each equilibrium point was found in XPPAUT using the software's implemented Newton's method to locate the steady state from a nearby initial condition and numerical Jacobian to calculate the eigenvalues. Which in turn allows us to determine the stability of each equilibrium point. The results of this process are shown, for default parameter values, in the table below.

Table1: Equilibrium Points of the Full Model		
EQ PT	Values	Stability
—	(A, M, E, p, B, I, G)	—
I	$(0, 0, 0, 0, 300, 10, 100)$	Stable
II	$(11.753, 7037.9, 1175.8, 0.058113, 296.54, 9.9452, 100.46)$	Unstable
III	$(255.31, 380.19, 74567, 1.6696, 134.34, 6.6152, 139.29)$	Unstable
IV	$(0, 0, 0, 0, 36.96, 2.8, 250)$	Unstable
V	$(95.607, 56437, 9565.7, 0.060949, 38.23, 2.8744, 246.18)$	Unstable
VI	$(262.89, 395.5779, 77913.936, 1.6648, 128.2, 6.3262, 144.12)$	Unstable
VII	$(0, 0, 0, 0, 0, 0, 600)$	Stable

In particular EQ PTs I, III, and VII are of interest to us. First EQ PT I has no elevated populations of immune system cells primed to target beta cells and has healthy values for beta cell mass, insulin concentration, and glucose level and therefore can be assumed to be the healthy steady state. Next we have EQ PT III, the healthy threshold steady state. We have given EQ PT III this name because despite having elevated populations of activated T-cells, memory cells, effector cells, and peptides beta cell mass, insulin concentration, and glucose levels remain at a healthy value. Last we have the diseased steady state, EQ PT VII. We know EQ PT VII is the diseased steady state because $B = 0$ immediately gives us $I = 0$ since there are no more beta cells to produce any insulin leaving $G = \frac{R_0}{E_{GO}} = 600$ as our steady state value for glucose. As for the impact this has on the rest of the model having no beta cell mass means that there are no beta cells to be killed and produce peptides which

is why we have $p = 0$ and since there are no more peptides to prime the T-cells to activate and seek out beta cells we have that $A = 0$ which implies that both $M = 0$ as well as $E = 0$ since there are no activated T-cells to become memory or effector cells.

Chapter 4: Results

4.1 Tristability and Bifurcation Analysis

We start by first presenting a theoretical method to avoid T1D by varying the death rate of peptides, δ_P, so that we end up in the healthy basin of attraction, the subset of the flow for (2.11) − (2.19) such that all trajectories converge to EQ PT I as $t \to \infty$. As we can see Figures 4.1 and 4.2 and especially when viewed from the B VS δ_P plane in Figure B.1 in Appendix 2 show us that for the approximate range of values $0 \leq \delta_P \leq 1$, that leads to tristability in the full model. To see how the tristability was established we start at $A = 500, M = 0, E = 1 \times 10^6, B = 300, I = 10$, and $G = 100$ and continue in δ_P until we reach a state of stable oscillation with $\delta_P = 1$. From here, we lower the death rate of peptides to 0.2 and continue in δ_P until we reach the nearest steady state, EQ PT III. From here we raise δ_P back to its default value of 1 and continue in δ_P until we reach stability again, this time at EQ PT I the healthy steady state. We also consider what happens when we start at the initial condition (0,0,0,0,0,600) with $\delta_P = 1$ and since glucose does not directly depend on peptide levels the diseased steady state undergoes no bifurcations and just remains a stable steady state as shown in figures 4.1, 4.2, and 2.1, thus showing tristability. This means that if we start at stable oscillations for default peptide death rates we can transition to the

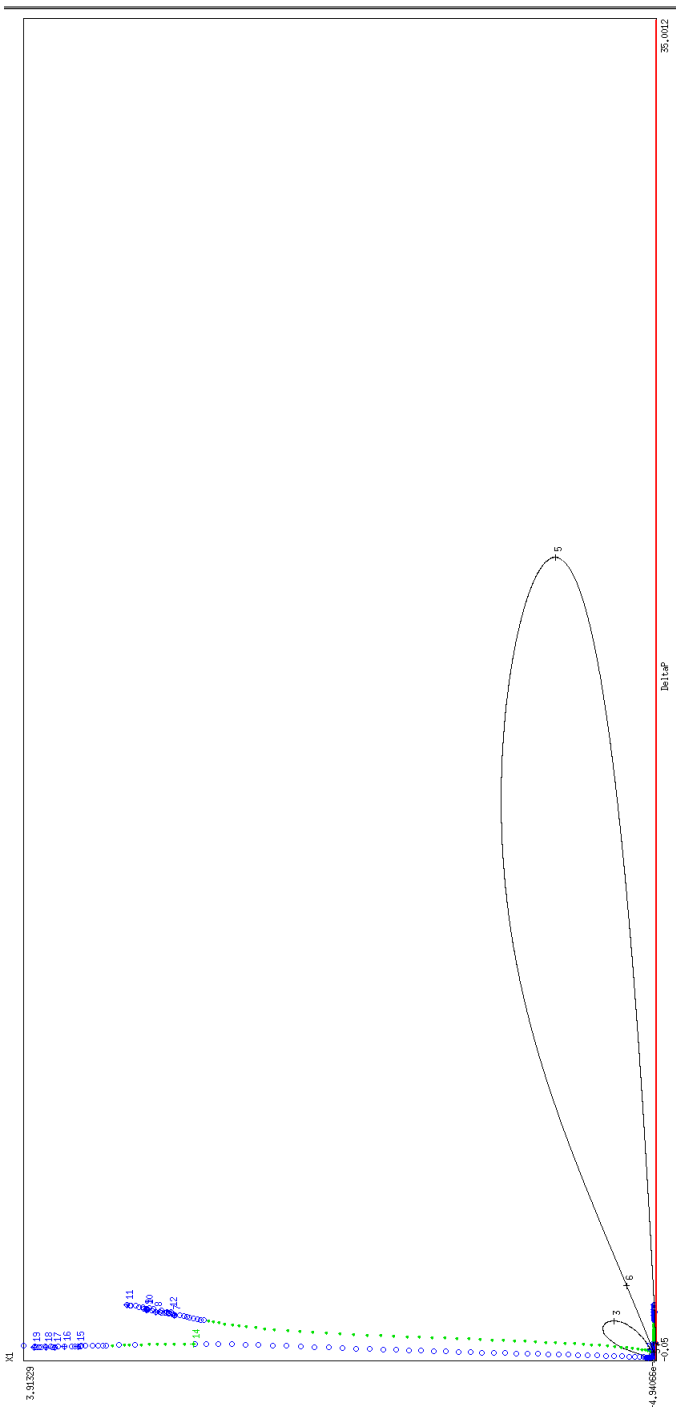

Figure 4.1: This figure is the bifurcation diagrams of EQ PT I, EQ PT III, and EQ PT VII with respect to $A = x_1$ as we vary the turn over rate of peptides, δ_P. The larger of the two loops seen is the path that EQ PT II and V take as they produce a saddle node bifurcation. The smaller of the two loops is the path that EQ PT III and VI take as they produce as saddle node bifurcation. Lastly the solid red line seen at the bottom is the path EQ PT VII takes. See Figure 4.2 for a detailed view of the two hopf bifurcations and the saddle node bifurcation of EQ PT I and EQ PT III.

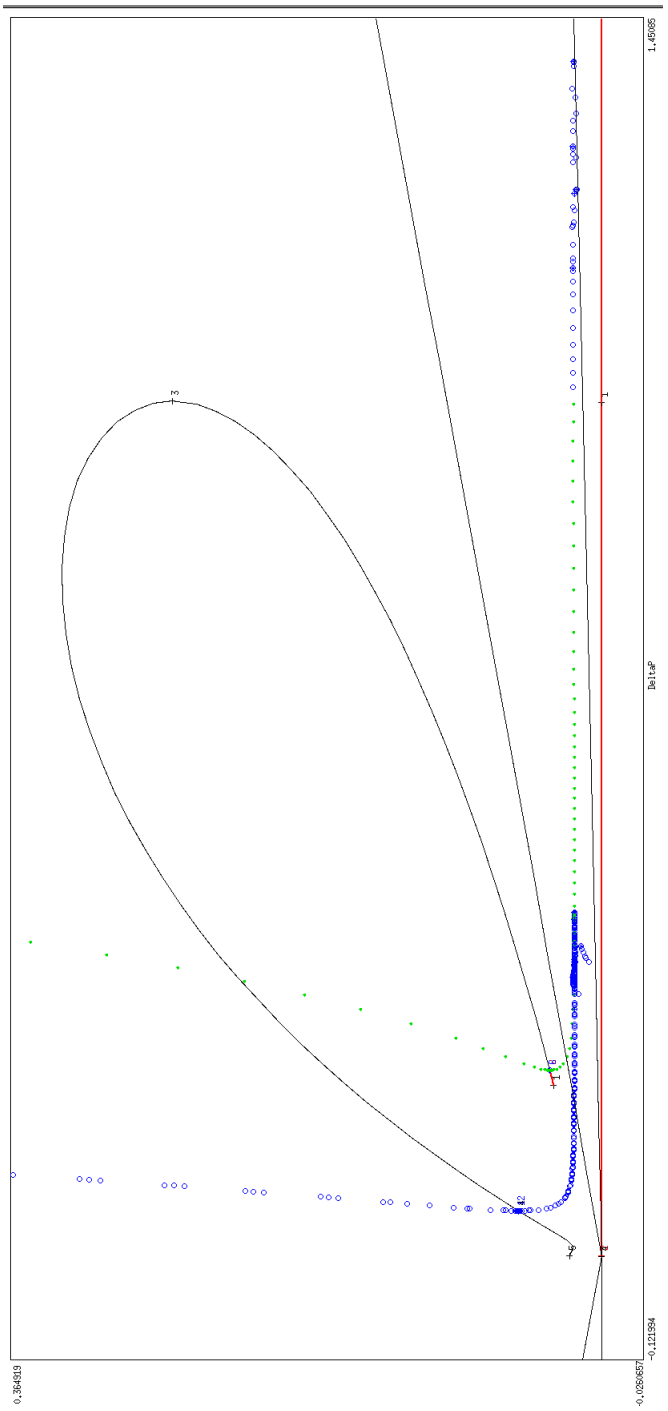

Figure 4.2: This figure is a closer view of figure 4.1. Here we can see where the Hopf bifurcations occur in EQ PT III (super critical) and in EQ PT V (sub critical). The figure shows the Saddle node bifurcations of EQ III and VI Note that negative values of δ_p are nonphysiological.

healthy basin of attraction by first lowering the death rate of peptides until the oscillatory behavior disappears for the new value of δ_P then by quickly raising it back to the default value $\delta_P = 1$ arrive in the healthy basin of attraction and thus avoiding the diseased basin of attraction all together.

4.2 Two Parameter Bifurcations

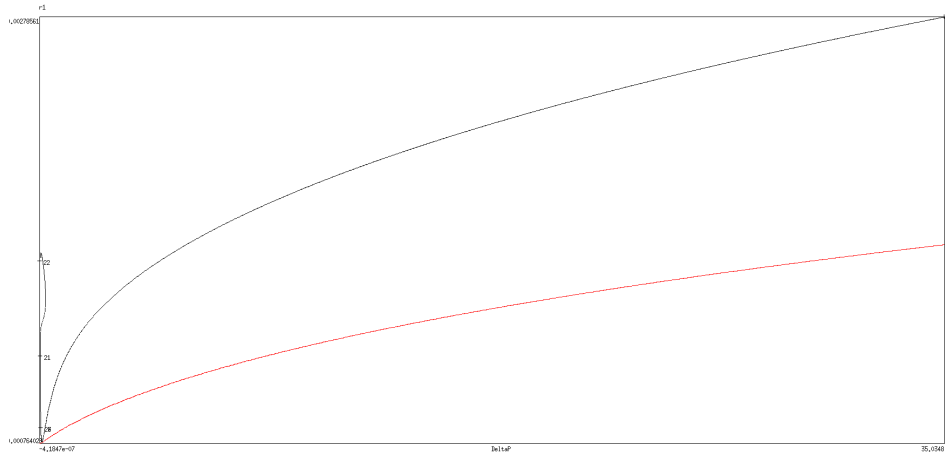

Figure 4.3: In black we see the continuation of EQ PT III's supercritical Hopf bifurcation and in red we see the continuation of the saddle-node bifurcation

For two parameter bifurcations, we are particularly interested in δ_P for the same reasons we have been up until now but also in the rate constant r_1 since any saddle-node bifurcations it undergoes represents a pathway to T1D [2]. We again turn our attention to EQ PT III and continue it in r_1 at its supercritical Hopf bifurcation and see two key things of interest, see Figure 4.3. The first is that EQ PT III now undergoes a Hopf-Hopf bifurcation as r_1 increases to $r_1 = 1.180437 \times 10^{-3}$. Next we continue EQ PT III at its Saddle-Node bifurcation in r_1 resulting in a Zero-Hopf bifurcation as seen in Figure 4.4. Now we continue EQ PT III's subcritical Hopf bifurcation in r_1 and obtain no new results indicating that while there is cyclic behavior these oscillations do not provide a new pathway nor get rid of an already

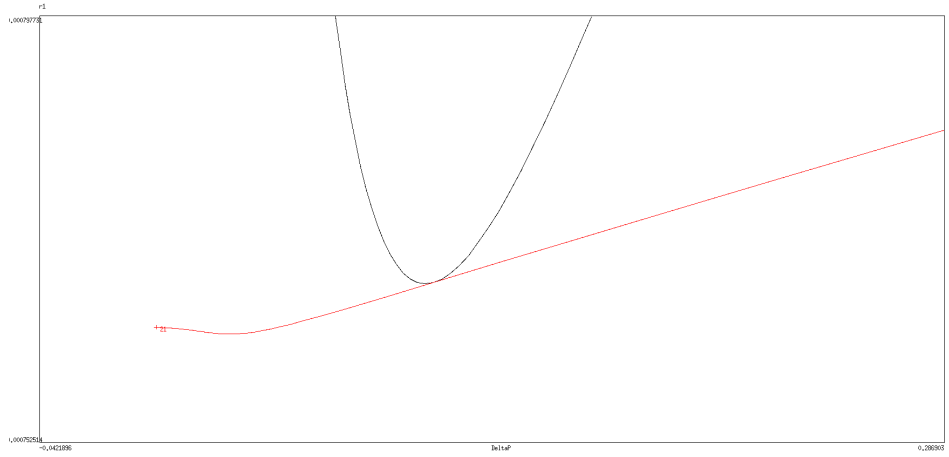

Figure 4.4: Here we see a close up of figure 4.3 showing a Zero-Hopf bifurcation at the tangential intersection of EQ PT III's supercritical Hopf bifurcation (in black) and its saddle-node bifurcation (in red).

existing pathway to T1D. See Figure 4.3

From here we continue EQ PT I at its Saddle-Node bifurcation in r_1 and find that its stability does not change as we alter r_1 and undergoes no further bifurcations with respect to r_1. However δ_P must increase in order to maintain the same dynamics.

Since the diseased steady state, EQ PT VII, is always stable independent of δ_P and r_1 continuing it in r_1 yielded no new results. However for small δ_P as r_1 increases we find additional dynamics connecting through EQ PT III.

4.3 Period Doubling

As is shown in Figures 4.3 and 4.5 by changing the values of δ_P and r_1 to 0.055812 and 0.001631 the combined model undergoes a period doubling bifurcation. It is in this range of values that oscillations also change from stable to unstable. As one can see from the figures mentioned above as well as Figure 4.6 as the A vs δ_P plane is shifted in the r_1 direction the Hopf bubble caused by the period doubling bifurcation appears. Figure 4.7 beta cell mass

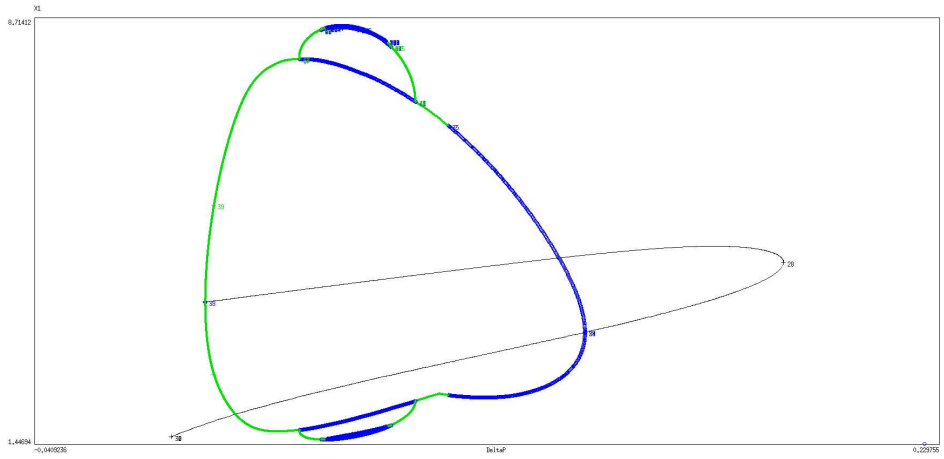

Figure 4.5: Period doubling cascade zoomed in. In blue we see unstable oscillations and in green we see stable oscillations.

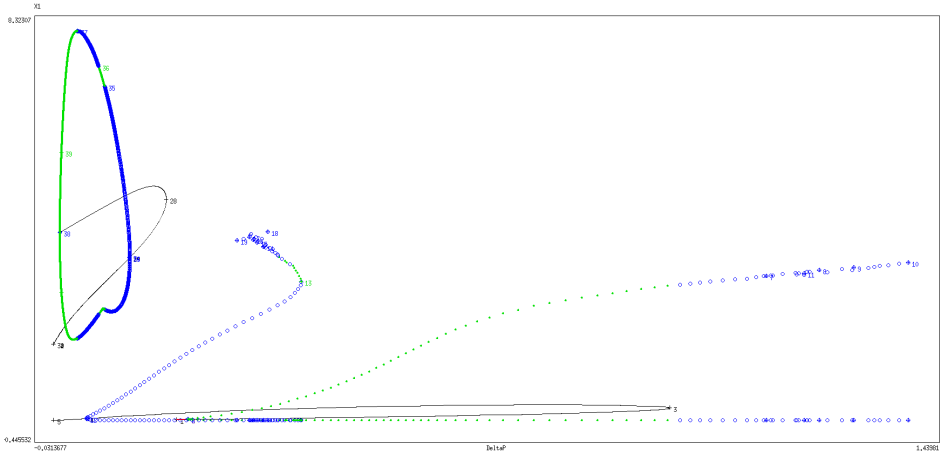

Figure 4.6: Period doubling cascade zoomed out after decreasing r_1 to obtain a period doubling bifurcation. This compares to Figure 4.2 but with much larger x_1-axis to capture the Hopf bubble and additional dynamics.

is severely impaired by this point in time due to the highly cyclic behavior of a very low peptide level as well as the increase in glucose-sensitive beta cell replication coefficient r_1. However since the range of parameters for this behavior is so small we conclude that it is of little biological importance.

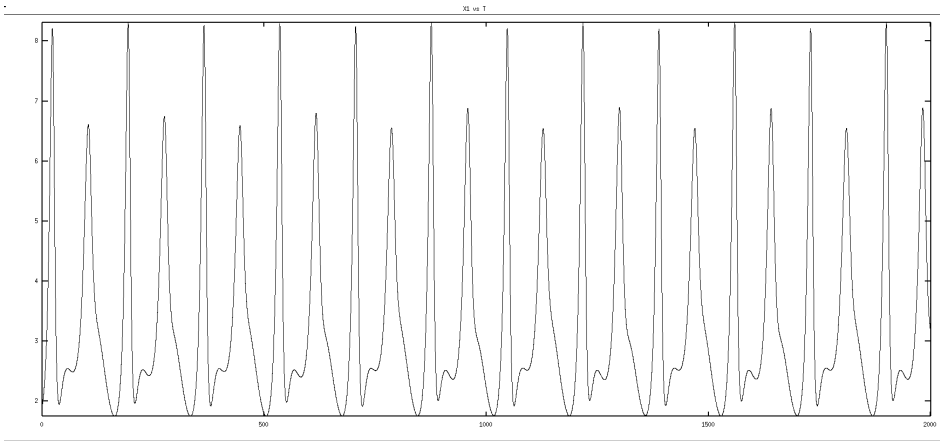

Figure 4.7: This is a period 8 oscillations corresponding to Figure 4.3. Activated T-cells vs Time (Days). In the dimensional model the range of values for activated T-cells would range from 2000 to about 8500. The parameters used to generate this figure were all default values except for the values of $\delta_P = 0.055812$ and $r_1 = 0.001631$.

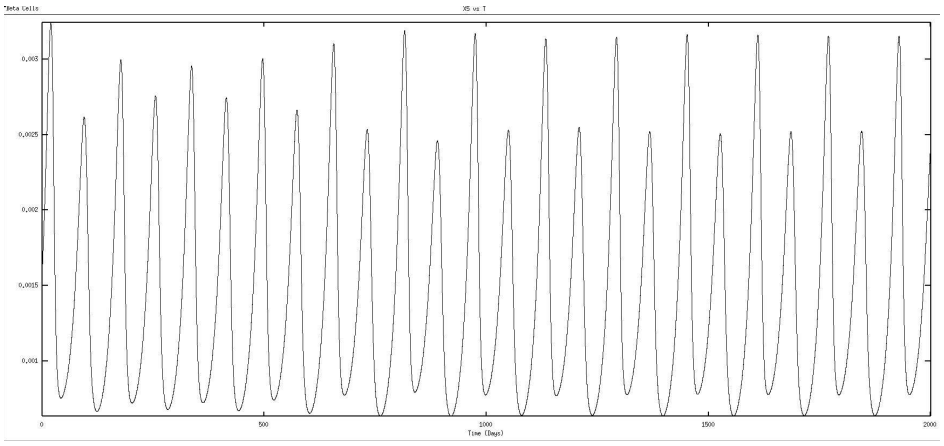

Figure 4.8: Beta cell mass oscillations for a very low level of beta cell mass in the nondimensional model as T1D finally sets in for this set of parameters. In the dimensional model the range of beta cell mass would be 0.3 to 1 mg. The corresponding glucose concentration would be approximately 587 mg/dl.

4.4 Beta Cell recovery

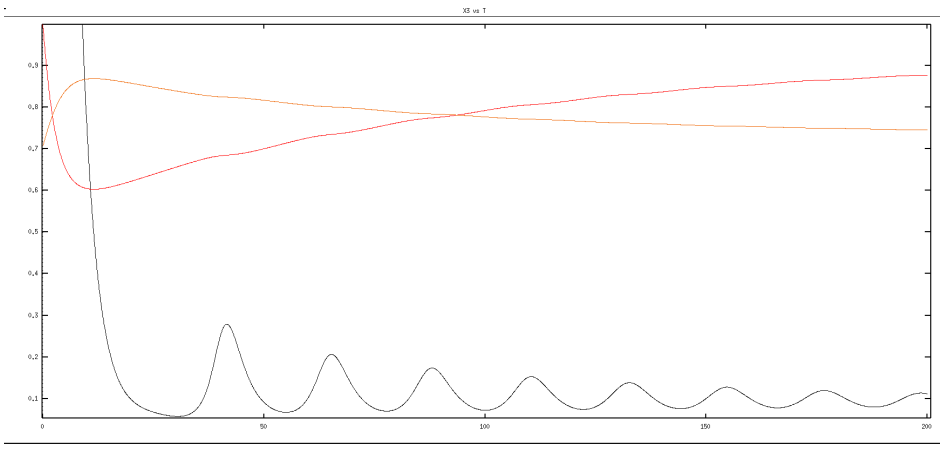

Figure 4.9: This fiure shows the cyclic recovery of beta cells and glucose levels for $\delta_P = 0.2$. With beta cell mass in red, glucose concentration in orange, and effector T-cell population in black versus time (Days)

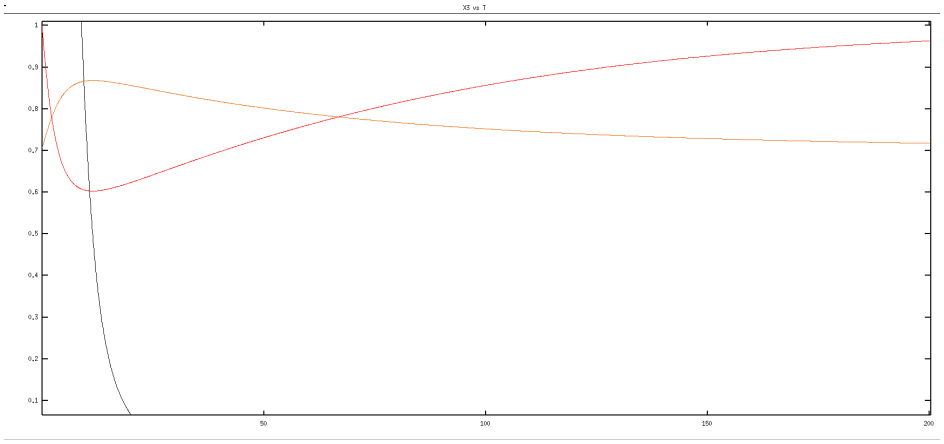

Figure 4.10: This figure shows the noncyclic recovery of Beta cell mass and glucose for elevated values of $\delta_P = 2$.With beta cell mass in red, glucose concentration in orange, and effector T-cell population in black versus time (Days)

As shown in Figure 4.9 for low values of δ_P ($\delta_P = 0.2$) the beta cell mass and glucose concentration return to the healthy steady state values, b=1 and g=0.70711 respectively

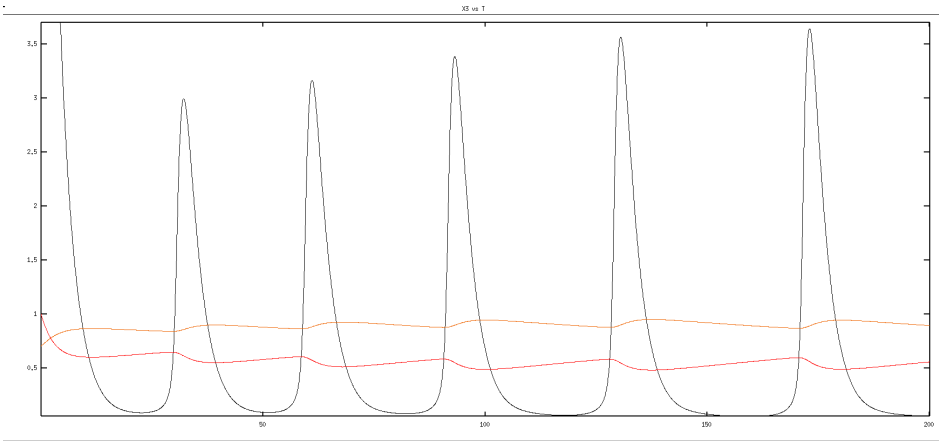

Figure 4.11: The cyclic pattern exhibited by T1D without the recovery of beta cell mass or glucose concentration. With beta cell mass in red, glucose concentration in orange, and effector T-cell population in black versus time (Days). The variables are from the nondimensional model

for the scaled model (2.20) − (2.28), while still showing the cyclic behavior of the immune system. This corresponds to a build up of the peptides needed to trigger the immune system to target beta cells but not enough effector T-cells to overwhelm the beta cells in the pancreas causing T1D. In Figure 4.10 we see that for high values of the peptide turnover rate ($\delta_P = 2$) we get noncyclic recovery from the attack on the beta cells by the immune system which corresponds to insufficient peptide levels to sustain the chronic nature of T1D and therefore lead to recovery. In Figure 4.11 we show the beta cells come under attack by the effector T-cells in cyclic oscillations but never recover.

4.5 Quasi-Steady State Assumptions

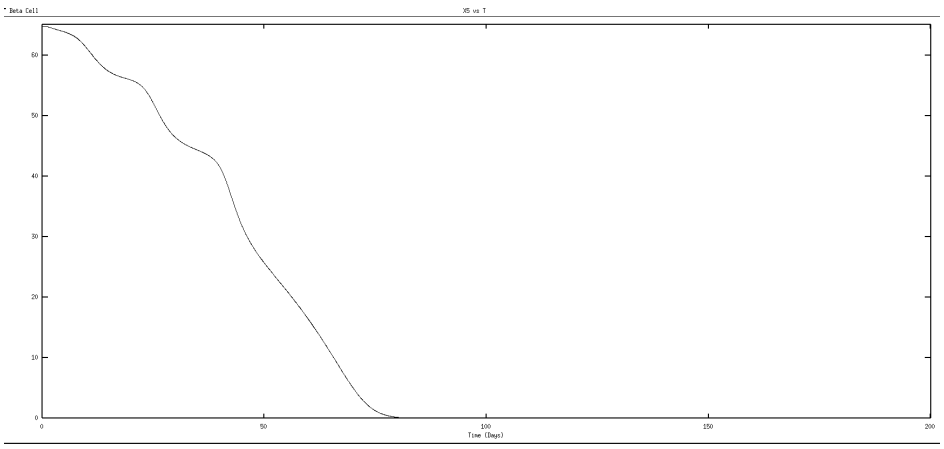

Figure 4.12: Here we see the dynamics of the beta cell mass without the peptide QSSA being made

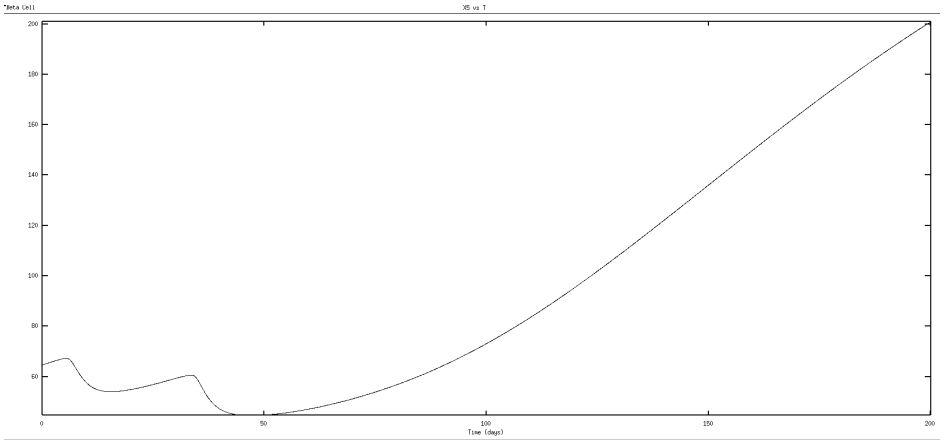

Figure 4.13: Here we see the beta cell mass dynamics with the peptide QSSA being made

The quasi-steady state assumption (QSSA) made in the Mahaffy Model $\frac{dp}{dt} = 0$ did not apply for the combined model. To see this scale both δ_P and R by 100 at an initial condition that is not a steady state and track the dynamics of the combined model with the assumption being made and then again without it being made, see Figures 4.11 and 4.12. However since parameters $c12$ and $c13$ are so large compared to the other parameters in the scaled model

there is another variable that we can use to make a QSSA. By setting $\frac{dI}{dt} = 0$ and solving for I we obtain $I(t) = \frac{\sigma_2}{k} B(t) \frac{G^2(t)}{\alpha_2 + G^2(t)}$. As one can see from Figures 15 and 16 the insulin QSSA is a valid assumption to make as it does not alter the behavior of the model for default parameters.

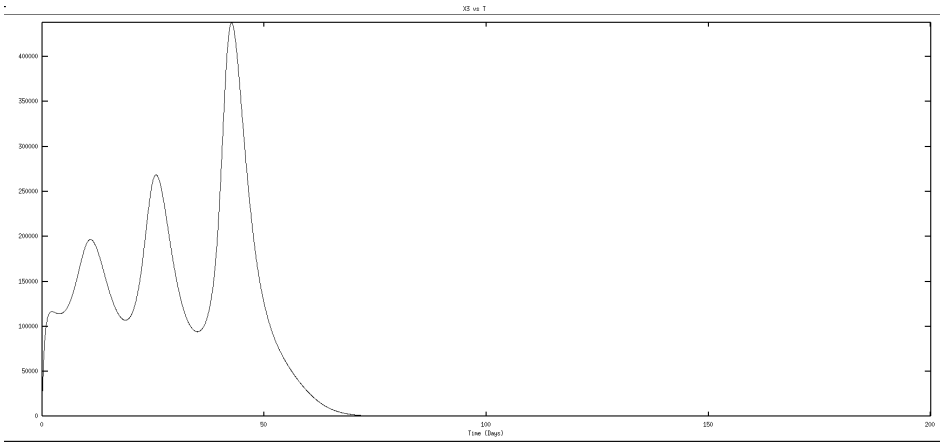

Figure 4.14: Full model without the Insulin QSSA being made showing E vs time (Days).

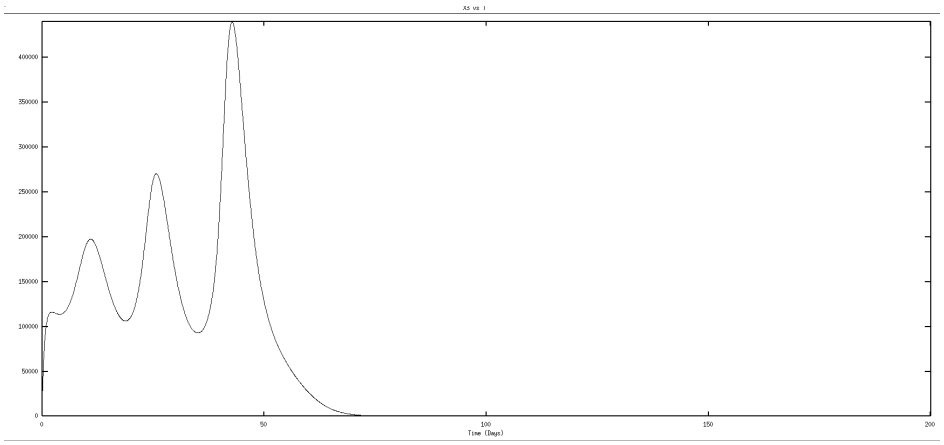

Figure 4.15: E vs Time (Days) with the insulin QSSA being made

Chapter 5: Discussion

As we have shown combining the Topp and Mahaffy models and allowing glucose values to feed back into the Mahaffy terms have allowed us to see both mathematical and biological behavior that is not only interesting but also important in understanding the nature of how T1D progresses and then eventually sets in. This is best illustrated in the recovery of beta cells for high enough values of peptide turnover rates. We are now also able to see the effect that peptides have on the cyclic behavior of the activation of T-cells and how that cyclic behavior undergoes period doubling. Our analysis of the tristability of the combined model suggests that it may be experimentally possible to control whether one ends up in the healthy basin of attraction or the diseased basin of attraction by starting at stable oscillations, then lowering the death rate of peptides until stable oscillations have stopped, and then suddenly raising δ_P back up to its default value of 1.

While more general versions of the Mahaffy and Topp Models exist these two were chosen instead of their more general counter parts for several reasons. For the Mahaffy Model our reasoning comes down to the time scale. The more general model proposed by Majid et al. [3] is a two clone model that models the onset of T1D but as stated in Topp et al. [2] a two clone model becomes more significant on the time scale of minutes instead of days. The Topp Model also has been generalized in two different ways Goel et al. [4]. The first way is by including an insulin degregation term, $-d_I I$ in the beta cell mass equation for when

there is a surplus of insulin signaling to the pancreas to lower beta cell mass. The second way is to also to treat the parameter for insulin sensitivity as a function of maximal insulin secretion per beta cell, hypersecretion of insulin. We did not consider these changes to the Topp model because the lack of insulin in T1D due to reduced beta cell mass likely makes these additional terms less important.

Appendix 1:

Below are four tables of parameters along with default values where appropriate. The first of these tables, Tables 1.1 and 1.2, are tables of default parameter values used in the full model presented above (2.11) - (2.19). The values in Tables 1.1 and 1.2 were obtained from Mahaffy et al. [1] and Topp et al. [2]. The parameter values for the Mahaffy parameters were obtained by taking the values in Table B2 in Mahaffy and solving for the original parameter values using the appropriate scalings given by Mahaffy. The third and fourth of these tables, Table 1.3 and 1.4, are the default values of the composite parameters used in the nondimensional model, (2.20)-(2.28),the fifth, Table 1.5, is a table of scalings used to obtain the nondimensionalized model, (2.20)-(2.28), and the sixth table, Table 1.6, is a table of both the independent variable and the dependent variables and their meanings.

Table 1.1:

Parameter	Default value	Meaning	Units
n	2	Hill coeff. for T cell activation	–
k_1	2	Peptide level for $\frac{1}{2}$ max activation	peptide units
$\hat{m}$	3	Hill coeff. for memory-cell production	–
$\hat{a}$	0.7	maximal fraction of memory cells produced	–
k_2	1	peptide level for $\frac{1}{2}$ max memory cells	peptide units
σ_1	20	influx of naive T cells from Thymus	$cellday^{-1}$
α_1	2	rate of production of A per M	day^{-1}
$\beta + \delta_A$	1	rate of cell division + death rate of activated T cells	day^{-1}
ϵ	1×10^{-3}	T cell competition parameter	$(cellday)^{-1}$
$\beta 2^{m_1}$	10	rate of cell division *times* maximum number of memory cells produced per proliferating T cell	day^{-1}
δ_M	0.01	death rate of memory T cells	day^{-1}
$\beta 2^{m_2}$	100	rate of cell division *times* number of effector cells produced per proliferating T cells	day^{-1}
δ_E	0.3	death rate of effector T cells	day^{-1}
R	$\frac{50}{300} \times 10^{-6}$	peptide accumulation rate	$day^{-1}cell^{-1}$

Table 1.2:

Parameter	Default value	Meaning	Units
δ_p	1	peptide turnover rate	day^{-1}
$\hat{k}$	0.14×10^{-6}	beta-cell killing per effector T cell	$day^{-1}cell^{-1}$
S	0.72	Total insulin sensitivity	$ml\mu U^{-1}day^{-1}$
E_{GO}	1.44	Total glucose effectiveness at zero insulin	day^{-1}
R_0	864	net rate of glucose production at zero glucose	$mgdl^{-1}day^{-1}$
σ_2	43.2	maximum rate of insulin secretion per beta cell	$\mu Uml^{-1}day^{-1}$
α_2	20000	half max of the sigmoid $\frac{G^2}{\alpha_2+G^2}$ squared	mg^2dl^2
k	432	combined insulin uptake at the liver, kidneys, and insulin receptors (insulin cleared)	day^{-1}
d_0	0.06	beta cell death rate at zero glucose	day^{-1}
r_1	0.84×10^{-3}	rate constant	$mg^{-1}dlday^{-1}$
r_2	0.24×10^{-5}	rate constant	$mg^{-2}dl^2day^{-1}$

Table 1.3:

Comp. Par.	Definition	Default value
c1	$\frac{\sigma_1 \mathring{a}}{\bar{a}}$	0.02
c2	$\frac{\alpha_1 \mathring{a} \bar{m}}{\bar{a}}$	20
c3	$(\beta + \delta_A)\mathring{a}$	1
c4	$\alpha_1 \mathring{a}$	2
c5	$\delta_M \mathring{a}$	0.01
c6	$\delta_E \mathring{a}$	0.3
c7	$\delta_P \mathring{a}$	1
c8	$r_2 \mathring{a} \bar{g}^2$	0.048
c9	$r_1 \mathring{a} \bar{g}$	0.1188
c10	$d_0 \mathring{a}$	0.06
c11	$\kappa \mathring{a} \bar{e}$	0.014
c12	$\frac{\sigma_2 \bar{b} \mathring{a}}{\bar{i}}$	1296
c13	k	432
c14	$\frac{R_0 \mathring{a}}{\bar{g}}$	6.1094

Table 1.4:

Comp. Par.	Definition	Default value
c15	$E_{GO}\mathring{a}$	1.44
c16	$S\mathring{a}\bar{i}$	7.2
c17	n	2
c18	$\frac{k_1}{\bar{p}}$	0.4
c19	$\hat{a}$	0.7
c20	$\frac{k_2}{\bar{p}}$	0.2
c21	$\hat{m}$	3

Table 1.5:

Scaled Variable	Scaling	Definition	Default Value
t	$\mathring{a}$	—	1
A	$\bar{a}$	$\frac{1}{\epsilon\mathring{a}}$	1×10^3
M	$\bar{m}$	$\bar{a}\mathring{a}\beta 2^{m_1}$	1×10^4
E	$\bar{e}$	$\bar{a}\mathring{a}\beta 2^{m_2}$	1×10^5
p	$\bar{p}$	$R\mathring{a}\bar{e}\bar{b}$	5
B	$\bar{b}$	300	300
I	$\bar{i}$	10	10
G	$\bar{g}$	$\sqrt{\alpha_2}$	141.4214

Table 1.6:

Variable	Meaning	Units
A	Population of activated T cells at time t	cells
M	Population of memory T cells at time t	cells
E	Population of effector T cells at time t	cells
p	peptide level at time t	peptide levels
B	concentration of remaining beta cells per volume	mg/dl
I	Insulin	$\frac{\mu U}{ml}$
G	Concentration of glucose	mg/dl
t	time	days

Appendix 2:

This section is devoted to additional figures

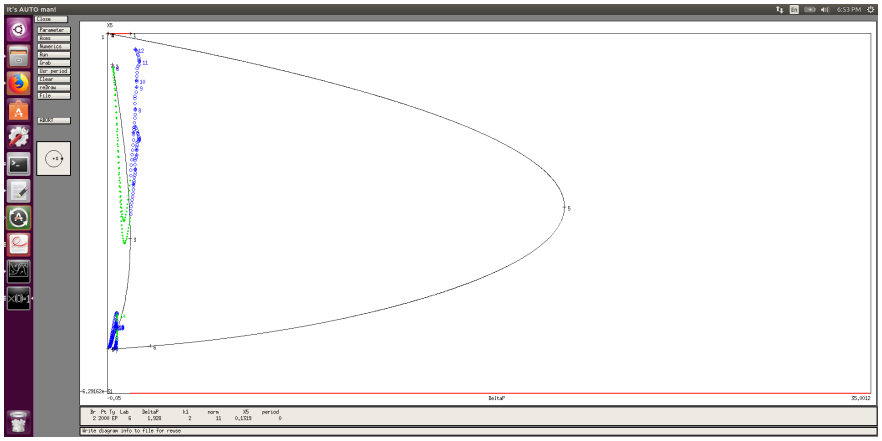

Figure 2.1: Bifurcation diagram showing tristability in the beta cell vs δ_P plane. Stable oscillation in green, unstable in blue. Stable steady state in red and unstable steady state in black

Appendix 3:

Below are the two matlab files used to find equilibrium points.

This is BetterEBPlots.m

```
%The parameters form Mahaffy below were
%calculated using Table B.2 however their values do not appear anywhere in
%the paper itself
% This coresponds to BetterFullModel.ode
clear all
clc
%this is the time scale
sa=1;
%Mahaffy parameters
n=2;
k1=2;
m=3;
a=0.7;
k2=1;
sigma1=20;
```

```
alpha1=2;

%beta=2;

%DeltaA=0.01;

%lamda1=(beta+deltaA)

Lamda1=1;

DeltaM=0.01;

DeltaE=0.3;

DeltaP=1;

epsilon=1e-3;

%M1=8;

%M2=60;

%Lamda2=beta*2^m1

Lamda2=10;

%Lamda3=beta*2^m2

Lamda3=100;

R=(50/300)*10^(-6);

kappa=0.14*10^(-6);

%Topp parameters

S=0.72;

EGO=1.44;

R0=864;

sigma2=43.2;

alpha2=20000;
```

```
k=432;
d0=0.06;
r2=0.24*10^(-5);
r1=0.84*10^(-3);

E=-1:5:1e5;
B=-1:0.5:306;
[e,b]=meshgrid(E,B);

%Below I define the functions used in the definitions of H(E,B) and B(E)
p=@(e,b) R*e.*b/DeltaP;

f1=@(e,b) p(e,b).^n./(k1^n+p(e,b).^n);
f2=@(e,b) a*k2^m./(k2^m+p(e,b).^m);
%Came from M'=beta2^m1f2*A-alpha1*f1*M-deltaM*M
coef1=@(e,b) Lamda2*f2(e,b)./(alpha1.*f1(e,b)+DeltaM);
%M=@(e,b) coef1(e,b)*A;

%these are the coefficents to be used to derive A(E,B)
coefa=-epsilon;
coefb=@(e,b) alpha1*coef1(e,b).*f1(e,b)-Lamda1;
coefc=@(e,b) sigma1*f1(e,b);
```

```
AP=@(e,b) (-coefb(e,b)+sqrt(coefb(e,b).^2-4*coefa*coefc(e,b)))/(2*coefa);
AM=@(e,b) (-coefb(e,b)-sqrt(coefb(e,b).^2-4*coefa*coefc(e,b)))/(2*coefa);
MP=@(e,b) coef1(e,b)*AP(e,b);
MM=@(e,b) coef1(e,b)*AM(e,b);

HP=@(e,b) Lamda3*(1-f2(e,b)).*AP(e,b)-DeltaE*e;
HM=@(e,b) Lamda3*(1-f2(e,b)).*AM(e,b)-DeltaE*e;

%I now define the functions to be used in deriving B(E)
CoeffA=-r2;
CoeffB=r1;
CoeffC=@(e) -d0-kappa*e;

GP=@(e) (-CoeffB+sqrt(CoeffB^2-4*CoeffA.*CoeffC(e)))/(2*CoeffA);
GM=@(e) (-CoeffB-sqrt(CoeffB^2-4*CoeffA.*CoeffC(e)))/(2*CoeffA);

% %0=R_0-(E_G0+S*I)*G
IP=@(e) 1/S*((R0./GP(e))-EGO);
IM=@(e) 1/S*((R0./GM(e))-EGO);

% %0=sigma2*B*G^2/(alpha2+G^2)-kI
BP=@(e) k*IP(e).*(alpha2+GP(e).^2).*((sigma2*(GP(e).^2)).^(-1));
BM=@(e) k*IM(e).*(alpha2+GM(e).^2)./(sigma2*(GM(e).^2));
```

```
contour(e,b,HP(e,b),[0,0],'ShowText','on','linecolor','r')
hold on
contour(e,b,HM(e,b),[0  0],'ShowText','on','linecolor','k')
hold on

e=-1:5:1e5;
%These two lines turn BP and BM into fixed vectors
BPv=BP(e);
BMv=BM(e);
%This line assigns a logical to each value of BP. It returns 1 for True
%values of BPv and returns a 0 for False if BPv is imaginary or complex
logind=BPv==real(BPv);
plot(e(logind),BPv(logind),'b',e(logind),BMv(logind),'r')
% plot(e,BP(e),'b')
% hold on
% plot(e,BM(e),'r')
title('B(E) VS H(E,B)=0')
%zlabel('H_Plus')
xlabel('E')
ylabel('B')
%legend('BP','BM','H')
%
```

```
%%%axis([x y z])
%%axis([-0.05 1 -1 400])
```

This is BetterZeros.m

```
%This is the code that finds the zeros of H in BetterEBPlots.m in this code
%B is treated as a parameter and this code should mimic the code in
%practice.m the value guessed for B should be based on the figure produced
%by BetterEBPlots.m
clear all
clc
format long


%time scale
sa=1;
%Mahaffy parameters
n=2;
k1=2;
m=3;
a=0.7;
k2=1;
sigma1=20;
alpha1=2;
%beta=2;
%DeltaA=0.01;
```

```
%lamda1=(beta+deltaA)

Lamda1=1;

DeltaM=0.01;

DeltaE=0.3;

DeltaP=0.2;

epsilon=1e-3;

%M1=8;

%M2=60;

%Lamda2=beta*2^m1

Lamda2=10;

%Lamda3=beta*2^m2

Lamda3=100;

R=(50/300)*10^(-6);

kappa=0.14*10^(-6);

a16=0.1;

%Topp parameters

S=0.72;

EGO=1.44;

R0=864;

sigma2=43.2;

alpha2=20000;

k=432;

d0=0.06;
```

```
r2=0.24*10^(-5);
r1=0.84*10^(-3);
%the parameter b use this as your guess based on the figure produced in
%BetterEBPlots.m
b=44.5;

e=0:15:6*10^(5);

p=@(e) R*e.*b/DeltaP;

f1=@(e) p(e).^n./(k1^n+p(e).^n);
f2=@(e) a*k2^m./(k2^m+p(e).^m);
%Came from M'=beta2^m1f2*A-alpha1*f1*M-deltaM*M
coef1=@(e) Lamda2*f2(e)./(alpha1.*f1(e)+DeltaM);
M=@(e) coef1(e)*A;

%these are the coefficents to be used to derive A(E,B)
coefa=-epsilon;
coefb=@(e) alpha1*coef1(e).*f1(e)-Lamda1;
coefc=@(e) sigma1*f1(e);

AP=@(e) (-coefb(e)+sqrt(coefb(e).^2-4*coefa*coefc(e)))/(2*coefa);
AM=@(e) (-coefb(e)-sqrt(coefb(e).^2-4*coefa*coefc(e)))/(2*coefa);
```

```
HP=@(e) Lamda3*(1-f2(e)).*AP(e)-DeltaE*e;

HM=@(e) Lamda3*(1-f2(e)).*AM(e)-DeltaE*e;


%initial guess of E for fsolve

e0=4.66e4;


%The stuff needed to plot solution curves

e=0:15:6*10^(5);

% plot(e,HP(e),'r')

% hold on

% plot(e,HM(e),'b')

% xlabel('E')

% ylabel('H')

% axis([-100 4e4 -4500 2e5])

% legend('HP','HM')

%title('Plots of H(E,300)')

%the awnsers

%e=fzero(HP,e0)

e=fzero(HM,e0)
```

Bibliography

[1] Joseph M. Mahaffy Leah Edelstein-Keshet, *Modeling Cyclic Waves of Circulating T Cells In Autoimmune Diabetes.* ociety for Industrial and Applied Mathematics,volume 67,number 4,pages 915-937, https://doi.org/10.1137/060661144

[2] Brian Topp, *A Model of β-Cell Mass, Insulin, and Glucose Kinetics: Pathways to Diabetes.* Journal of Theoretical Biology 2000, volume 206, number 4, pages 605-619 doi:10.1006/jtbi.2000.2150

[3] Majid Jaberi-Douraki, Massimo Pietropaolo, Anmar Khadra. emphPredictive Models of Type 1 Diabetes Progression: Understanding T-Cell Cycles and Their Implications on Autoantibody Release. http://journals.plos.org/plosone/article?id=10.1371/journal.pone.0093326

[4] Pranay Goel. emphInsulin Resistance or Hypersecreation? The βIG Picture Revistited. Journal of Theoretical Biology, 2015, volume 384 pages 131-139 https://doi.org/10.1016/j.jtbi.2015.07.033